Accepted Manuscript

Implementation of DEIS for reliable fault monitoring and detection in PEMFC single cells and stacks

K. Darowicki, E. Janicka, M. Mielniczek, A. Zielinski, L. Gawel, J. Mitzel, J. Hunger

PII:	S0013-4686(18)32092-9
DOI:	10.1016/j.electacta.2018.09.105
Reference:	EA 32637
To appear in:	*Electrochimica Acta*
Received Date:	07 May 2018
Accepted Date:	15 September 2018

Please cite this article as: K. Darowicki, E. Janicka, M. Mielniczek, A. Zielinski, L. Gawel, J. Mitzel, J. Hunger, Implementation of DEIS for reliable fault monitoring and detection in PEMFC single cells and stacks, *Electrochimica Acta* (2018), doi: 10.1016/j.electacta.2018.09.105

Implementation of DEIS for reliable fault monitoring and detection in PEMFC single cells and stacks

K. Darowicki[(1)], E. Janicka[(1)]*, M. Mielniczek[(1)], A. Zielinski[(1)], L. Gawel[1)], J. Mitzel[(2)] , J. Hunger[(3)]

[(1)] Department of Electrochemistry, Corrosion and Materials Engineering
Chemical Faculty, Gdansk University of Technology
11/12 Narutowicza, 80-233 Gdansk, POLAND

[(2)] German Aerospace Center (DLR), Institute of Engineering Thermodynamics
Pfaffenwaldring 38-40, 70569 Stuttgart, GERMANY

[(3)] Zentrum für Sonnenenergie- und Wasserstoff-Forschung Baden-Württemberg (ZSW)
Helmholtzstraße 8, 89081 Ulm, GERMANY

Abstract

Dynamic Electrochemical Impedance Spectroscopy (DEIS) was presented as novel method for diagnostic and monitoring of PEMFC stack and single cells operation. Impedance characteristics were obtained simultaneously with current - voltage characteristics for stack and each individual cell. Impedance measurements were performed in galvanodynamic mode. It allowed to compare performance of each cell and identification of faulty cell operation for activation, ohmic and mass transfer losses regions. The biggest difference in impedance value between healthy and faulty cell was registered for mass transfer losses region. The authors discussed the statistical selection of an equivalent circuit based on the course of χ^2 value in the function of current.

Keywords: PEM Fuel Cell; Performance; Diagnostics; Impedance; Equivalent Circuit

1. Introduction

Proton Exchange Membrane Fuel Cells (PEMFC) are already used in many areas of our lives. They are successfully applied as energy sources in stationary [1,2], mobile [3,4] and transport applications [5,6]. According to the assumptions specified in the report "Electrical Vehicles in Europe" of the European Environment Agency from 2016, it is planned to decrease share of cars with combustion engine by half in city transport by 2030 and to completely withdraw combustion engine cars from cities by 2050. These actions are aimed to reduce emission of greenhouse gas by 85-90% to 2050. According to the U.S. Department of Energy, sale of fuel cell cars increased 7 times during one year (February 2016 - February 2017). However, mass use of fuel cell stacks is still limited because of the following issues: lifetime, cost and efficiency of energy conversion. Those issues depend on many

*Corresponding author
E-mail address: ewa.janicka@pg.edu.pl
Phone number: +48 583471440
Postal address: Chemical Faculty, Gdansk University of Technology, 11/12 Narutowicza, 80-233 Gdańsk POLAND

factors such as design and assembly of stack, degradation of electrodes materials, operation parameters or contaminations. Many research teams try to improve the efficiency of cells in various ways, including developing new membrane materials with improved conductivity, chemical and mechanical strength [7–10], improving optimization process [11–13] or developing new diagnostic methods [14–16]. In order to reduce costs and increase performance of fuel cell, it is necessary to not only fully understand influence of working parameters on conversion efficiency, but also to know, how they affect fuel cell lifetime. To achieve this aim it is necessary to use reliable diagnostic method, which can give full characteristic of occurring processes in relatively short time.

Cell voltage monitoring (CVM) [17], total harmonic distortion (THD) measurements [18] and electrochemical impedance spectroscopy (EIS) [19] are the methods currently used in investigation of the operation of fuel cells. CVM is the most common method employed in fuel cell systems. It is simple and easy for implementation, but unfortunately it does not give full characteristic of occurring processes. THD is more complex method, but as for now practical applications are limited to stack level without characterization of single cells [20]. EIS provides the most valuable information, which allows identifying fuel cell failure. It allows distinguishing the processes responsible for voltage drop, which can be caused by activation, ohmic or mass transfer losses [21]. The activation losses depend on catalyst layer properties such as loading, type, utilization, electrochemically active area and stability of carbon support. The ohmic losses are dependent on conductivity and thickness of membrane, contact resistance between membrane electrode assembly (MEA) sublayers, compression pressure and electronic conductivity [22,23]. The mass transfer losses are connected with limited diffusion of reagents to catalyst layer, what is associated with size and number of pores in each layer, polytetrafluoroethylene percentage and interfacial gaps. Furthermore, the mass transport losses can be linked to liquid water accumulation in fuel cells.

Impedance measurements carried out in the traditional way belong to the canon of electrochemical tests. EIS method is perfect tool to characterization of fuel cell components including membrane [24–26] and electrode materials [27–29]. EIS is also used for investigation of PEMFC operation, but not without some limitations [30–32]. One of them is the requirement of stationarity of the tested object. However, changes in system behavior can be a natural result of the experiment (for example, change in potential in a galvanostatic experiment). On the other hand, in many cases the measuring technique is inherently non-stationary as in the case of measurements presented in this work. The current-voltage characteristic shows changes in the resistance of the fuel cell, thus reflecting the dynamic changes in the behavior of the tested system. Impedance measurement is a natural complement to the recording of current-voltage characteristics because it allows the separation of changes in individual components of the total impedance of the cell. Unfortunately, in the traditional approach using frequency response analysis (FRA) mode, the acquisition of a single spectrum requires a time equal to at least the sum of the inverse of all frequencies included in the spectrum.

It is expected that a good diagnostic method is going to provide the maximum number of information about working stack in the shortest possible time. Fast and reliable method is needed to improve performance and lifetime of fuel cells. Considering dynamic character of the changes occurring in working fuel cell system, the authors propose the DEIS method. This method uses a multi-frequency perturbation signal. It consists of number of elementary signals with different frequencies, amplitudes and phase shifts. By using the superposition of sinusoidal stimulations, the theoretical total impedance acquisition time is reduced to the period of the component of lowest frequency. Increased time efficiency is not the only justification for using the DEIS technique. Due to the fact that the properties of the tested cell change at a certain rate in a smooth manner with a change in load, it is not possible to obtain a frequency spectrum for each current value. Acquisition of only a single impedance value is possible. Because the load changes in time in a programmed step-wise or continuous way, changing the frequency of the perturbation signal would require stopping the process of load change which is in clear contradiction to the idea of recording the current-voltage curves.

Presented method is suitable for diagnostics of faulty working fuel cell, what allows for counteraction with respect to the occurring fault. The main reason of using the DEIS method is possibility of its implementation in real system. Limiting a measurement to 1Hz allows registration of impedance spectrum in 1s, what is significant improvement comparing to the EIS method. Using classic EIS method with frequency by frequency perturbation signal with the same frequency range time of measurement is at least 34 times longer. Comparison of exemplary results used with EIS and DEIS technique together with their technical implication were presented in the work of Wysocka et al. [33]. DEIS allows registration of fast changes, which makes it possible to perform measurements in real operating conditions. The DEIS method can be used also with lower frequencies in order to provide full characteristics of PEMFC, but measurement time needs to be adjusted with respect to the lowest frequency. The DEIS method was successfully implemented in corrosion detection [34–36], characterization of electrode materials [37,38] and direct methanol fuel cell monitoring [39,40].

2. Experimental

A test bench developed by the Fuel Cell Technologies Inc. was used to control and to maintain operating conditions and load. The measurements were conducted in nominal working conditions suggested by the manufacturer (see Table 1). Temperature of stack, pressure and humidity of reagents were stable. Flow rates were changed depending on the magnitude of load in order to maintain constant stoichiometry values. All parameters were controlled according to the guidelines for reliable PEMFC stack testing defined in the European Stack Test project [41,42].

Table 1. Nominal operating conditions of PEMFC stack.

Stack Temperature [°C]	Air Pressure [kPa_{abs}]	Hydrogen Pressure [kPa_{abs}]	Stoichiometry of Oxidant [-]	Stoichiometry of Fuel [-]	Relative Humidity of Air [%]	Relative Humidity of Hydrogen [%]
80	150	150	2.0	1.5	50	50

Hydrogen 5.0 (99.999% purity) and compressed ambient air were used for fuel and oxidant, respectively. The laboratory-examined PEMFC stack was supplied by the Zentrum für Sonnenenergie- und Wasserstoff-Forschung Baden-Württemberg - ZSW (Ulm, Germany). The stack consisted of ten single cells with an active geometrical surface area of 96 cm^2 each. A commercially available 7-layer MEA from the Greenerity, H500 Generation 3, was used for stack assembling. The flow channels were located in bipolar plates in cascaded flow field design configuration with parallel-connected multiple serpentine groups.

A system based on the test bench and two National Instruments modules (generating and acquisition ones) – PXIe-6124 and PXIe-4497 was used to obtain impedance spectra. Every single cell was monitored in a 2-electrode setup in galvanodynamic mode. A scheme of the tested stack of fuel cells was presented in Fig. 1.

Load was changed linearly with the rate of 20 mA s^{-1}, in the range from 0.04 to 1 A cm^{-2}. Multi-sinusoidal AC signal in the frequency range from 5 Hz to 1.2 kHz was used as an perturbation signal. The perturbation signal was optimized [43] to avoid overlapping of the peaks of single frequencies. During measurement an amplitude was regulated to maintain its value in the range from 5 to 10 % of the DC load. The use of multi-sinusoidal perturbation signal allowed studying a dynamic system like PEMFC, which exhibits stationarity within a measurement window of 1s. Obtained results were divided into 1-second fragments called “analysis windows”, which were decomposed and analysed using STFT (Short-Time Fourier Transformation).

3.Results and Discussion

3.1 Electrochemical measurements

The impedance spectra for the whole stack and each cell separately were recorded simultaneously with a current - voltage (I-V) characteristic. Fig. 2a presents voltage versus current density during linear change of load. Three characteristic regions can be distinguished according to the dominant causes for performance losses: activation losses, ohmic losses and mass transfer losses. An activation losses region can be observed up to 0.1 A cm^{-2}. For current densities between 0.1 A cm^{-2} and 0.6 A cm^{-2}, there is an ohmic losses region, which is preferred for stationary fuel cell operation and for long lifetime. Severe voltage fluctuation can be observed above 0.6 A cm^{-2}, which can be caused by liquid

water accumulation associated with high load and high water production within the cells. In this region voltage losses are mainly related to mass transport to reactive area. Individual cells voltage monitoring shows that the highest performance loss is registered for the cell no. 1 (Fig. 2b). The observed voltage drop in this cell can have various sources e.g. decreased active area of catalyst, low membrane humidification and reduced reactant flow in this cell. It is not possible to identify the causes only by analysis of voltage/current density characteristics of individual cells, because lower efficiency can have various sources [44]. More information can only be obtained by impedance analysis of the stack and single cells.

The DEIS spectra obtained for the stack (Fig. 2c) demonstrated that the biggest arc diameter corresponded to the lowest load. Diameter of impedance arc is decreasing with increasing current in the activation region. The minimum impedance value is characteristic for the ohmic losses area. Starting from the current density of 0.4 A cm^{-2}, slow linear increase in stack impedance can be seen. Simultaneously, the DEIS results were recorded for all cells corresponding to the stack. A comparison of the DEIS results for healthy and faulty cells are presented in Fig. 2d. Blue line corresponds to the results for the cell no. 7, which are typical for the properly working cells (cells no. 2 - 10). The healthy cells are characterized by bigger range of stable work conditions - 0.1 A cm^{-2} - 0.7 A cm^{-2}. After exceeding the mentioned value of current density the increase is less rapid than for the whole stack. Impedance characteristic of the cell no. 1 (Fig. 2d, black line) differs completely from the rest of cells and the stack. A diameter of the arc in Nyquist plot is much bigger and a continuous increase in impedance value is observed after exceeding the threshold values of the minimum flow rates specified by the stack manufacturer ZSW (3 L min^{-1} hydrogen and 10 L min^{-1} air). A comparison of healthy and faulty cells is presented in 3D graph (Fig. 2d).

The impedance characteristics corresponding to each loss region were isolated (according to the characteristics of the entire stack) from the comparison of the impedance diagrams of healthy and faulty cells. Fig. 3a presents the comparison of impedance spectra of the first and seventh cells in the region of activation losses. Both characteristics show a tendency to decrease the arc diameter as the load increases. Differences in the diameter of the arc for both cells are negligible, which may indicate that the lower efficiency of the first cell is not directly related to the electrochemical active surface of the catalyst. For 0.05 A cm^{-2} impedance value of faulty cell is around 20% higher than the healthy one. Analysing the region of ohmic losses, it can be seen that for the faulty cell it is practically three times shorter than for the healthy one. After exceeding set minimum flow rates of reagents, a continuous increase in the impedance value of the first cell is observed, while for the impedance diagram of the seventh cell in the region of ohmic losses, the size and shape of the arc do not change (Fig. 3b). For 0.35 A cm^{-2}, which is middle value of ohmic losses region (according to stack), impedance of faulty cell is nearly 3 times higher than the healthy cell. The rapid increase in the

impedance value of the faulty cell indicates a restricted transport of reagents to the catalytic layer, which often indicates that the cell is flooded with liquid water when current and water production increases [23]. On the DEIS graph of healthy cell the problem with mass transport becomes apparent only after exceeding the current density value of 0.7 - 0.8 A cm^{-2} (Fig. 3c). Measured difference in impedance value for current density of 0.8 A cm^{-2} between healthy and faulty cell is the biggest, it is around 5 times higher for faulty cell. The losses associated with mass transport are visible for the healthy cell at much higher density of applied current than for the faulty cell, however with a similar voltage of the cell. In this region, the impedance value determined for the malfunctioning cell does not change. Studies conducted with the use of EIS confirm that in the low frequencies range impedance spectra are related with reagents transfer to catalyst area [45–47]. Correctly chosen equivalent circuit is necessary for proper analysis of obtained impedance spectra.

3.2 Selection of equivalent circuit

Impedance description of phenomena occurring in fuel cells is usually performed using resistive and capacitive elements showing activation losses on cathode and anode. Additional elements are used to present ohmic part [32]. This approach makes it possible from the phenomenological point of view to reconstitute the impedance spectrum, taking into account the response of individual elements of the fuel cell [48]. On the other hand, it is sometimes impossible to justify some discrepancies between the empirical spectra and the adopted model [32]. As an example, the occurrence of areas of inductive loops in spectrum, which are explained by side reactions of intermediate products [49] or water transport inside the catalyst layer [50] can be cited. Hosseini and Zardari [51] draw attention to the existence of phenomena related to adsorption on the surface of catalysts and their impact on impedance results. Also modelling the behaviour of the fuel cell based on its structure and theoretical description of the processes occurring [52] suggests a more complex topology of the equivalent circuit.

The study of Springer et al. [53] indicates the need to consider transport processes in the cathodic area. In the report [54] a model of diffusion in a limited area was used to describe the phenomena occurring in the cathodic area. Attention was also drawn to the use of the constant phase element (CPE), which on one hand is justified by the porous structure of the electrodes but on the other hand has a significant impact on the values of other parameters that may cause them to be falsified. The satisfactory fitting of experimental data using CPE cannot be necessarily connected with the physical phenomena responsible for the impedance response of the system. The impedance circuits are not unambiguous, the low matching error value in the form χ^2 does not ensure that the model correctly reflects the physicochemistry of the system. Examples of the equivalent circuits with the same impedance response and definitely different topology can be found in the literature [55]. This indicates

the necessity to apply an additional verification methodology. It can be a complementary measurement technique and take into account other than statistical criteria during designing of an equivalent circuit.

Mentioned above complexity of phenomena that may affect the shape of impedance spectra requires caution while choosing an equivalent circuit and the meaning of individual elements placed in it. In this study, the authors focused on comparing the results of modelling with the use of various equivalent circuits, particularly taking into account statistics. As a measure of the quality of the match, the variability of χ^2 statistic, being the residual error of data matching process, was assumed. For comparative purposes, three most frequently proposed equivalent circuits for EIS analysis [55] and new equivalent circuits suggested by the authors of the presented paper were used. Fig. 4 shows the equivalent circuits used for analysis with χ^2 (i) relationship. Five topologies of equivalent circuits were used in the comparison. Two equivalent circuits, the most commonly used in the literature are variants a) and b) [19]. Both of them correspond to one of the most popular modeling approaches with a clear division into the influence of cathode and anode processes and phenomena related to electrolyte conductivity. The introduction of CPEs is justified by the variability of the capacity of the electric double layer along the pore depth in the case of porous electrode [45]. Model c) is based on the assumptions presented by the Conteau team, according to which Warburg impedance related to the diffusion resistance in the cathodic area should be taken into account [56]. The circuits shown in Figs. d) and e) are proposed by the authors, being models similar to those presented in [51] with limited diffusion impedance element. During the data fitting, two models were considered, with the presence and absence of CPE.

The best statistical fitting of equivalent circuit based on comparison of chi square value in the function of current in the regions of activation and ohmic losses is exhibited by two equivalent circuits d and e, presented in Fig. 4. The equivalent circuit with C element is characterized by stable fitting for the entire load range. It should also be noted that there is a small difference between the quality of matching in the last two cases (d) and (e). It can indicate a small effect of the use of CPE with correctly selected structure of other circuit components. For previously mentioned reasons, regarding the numerical falsification of the matching quality by CPE, the low value χ^2 observed using traditional capacitive elements may indicate the possibility of simplifying the impedance description.

4. Conclusions

The DEIS method presented in this paper was successfully used to diagnose the cell responsible for the reduced efficiency of the entire stack. The diagnostic method proposed by the authors makes it possible to obtain simultaneously impedances of individual cells and of the entire stack in the function of variable operation parameters in a dynamical system, such as a stack under changes of electrical load. The use of the proposed, preferred in statistical terms, equivalent circuit will allow obtaining a data library of parameter values under varying stack operation conditions. This will enable not only

diagnostics of malfunctioning cells but also identification of failure sources. Implementation of the proposed method will give information whether the failure is reversible or it is associated with poor operation optimization, which will enable appropriate reaction.

5. Acknowledgements

The research leading to the presented results has received funding from The National Center For Research and Development (NCBR, Poland) under Grand No. STAIR/6/2016 and the Federal Ministry of Education and Research (BMBF, Germany) Grant No.: 01LX1601. The work was realized in the COALA project (control algorithm and controller for increasing the efficiency of hybrid PEMFC systems in different applications) in the framework of the Polish-German Sustainability Research Call (STAIR II).

6. References

[1] C.A. Cottrell, S.E. Grasman, M. Thomas, K.B. Martin, J.W. Sheffield, Strategies for stationary and portable fuel cell markets, Int. J. Hydrog. Energy. 36 (2011) 7969–7975. doi:10.1016/j.ijhydene.2011.01.056.

[2] J. Hamelin, K. Agbossou, A. Laperrière, F. Laurencelle, T.. Bose, Dynamic behavior of a PEM fuel cell stack for stationary applications, Int. J. Hydrog. Energy. 26 (2001) 625–629. doi:10.1016/S0360-3199(00)00121-X.

[3] Y. Devrim, H. Devrim, I. Eroglu, Development of 500 W PEM fuel cell stack for portable power generators, Int. J. Hydrog. Energy. 40 (2015) 7707–7719. doi:10.1016/j.ijhydene.2015.02.005.

[4] F. Achmad, S.K. Kamarudin, W.R.W. Daud, E.H. Majlan, Passive direct methanol fuel cells for portable electronic devices, Appl. Energy. 88 (2011) 1681–1689. doi:10.1016/j.apenergy.2010.11.012.

[5] B. Allaoua, K. Asnoune, B. Mebarki, Energy management of PEM fuel cell/ supercapacitor hybrid power sources for an electric vehicle, Int. J. Hydrog. Energy. 42 (2017) 21158–21166. doi:10.1016/j.ijhydene.2017.06.209.

[6] Z. Hou, R. Wang, K. Wang, W. Shi, D. Xing, H. Jiang, Failure mode investigation of fuel cell for vehicle application, Front. Energy. 11 (2017) 318–325. doi:10.1007/s11708-017-0488-0.

[7] M. Vinothkannan, A.R. Kim, G. Gnana kumar, D.J. Yoo, Sulfonated graphene oxide/Nafion composite membranes for high temperature and low humidity proton exchange membrane fuel cells, RSC Adv. 8 (2018) 7494–7508. doi:10.1039/C7RA12768E.

[8] M. Vinothkannan, A.R. Kim, G. Gnana kumar, J.-M. Yoon, D.J. Yoo, Toward improved mechanical strength, oxidative stability and proton conductivity of an aligned quadratic hybrid (SPEEK/FPAPB/Fe_3O_4-FGO) membrane for application in high temperature and low humidity fuel cells, RSC Adv. 7 (2017) 39034–39048. doi:10.1039/C7RA07063B.

[9] A. Sahin, The development of Speek/Pva/Teos blend membrane for proton exchange membrane fuel cells, Electrochimica Acta. 271 (2018) 127–136. doi:10.1016/j.electacta.2018.03.145.

[10] M. Gil, X. Ji, X. Li, H. Na, J. Eric Hampsey, Y. Lu, Direct synthesis of sulfonated aromatic poly(ether ether ketone) proton exchange membranes for fuel cell applications, J. Membr. Sci. 234 (2004) 75–81. doi:10.1016/j.memsci.2003.12.021.

[11] B. Wang, H. Deng, K. Jiao, Purge strategy optimization of proton exchange membrane fuel cell with anode recirculation, Appl. Energy. 225 (2018) 1–13. doi:10.1016/j.apenergy.2018.04.058.

[12] P. Liang, D. Qiu, L. Peng, P. Yi, X. Lai, J. Ni, Contact resistance prediction of proton exchange membrane fuel cell considering fabrication characteristics of metallic bipolar plates, Energy Convers. Manag. 169 (2018) 334–344. doi:10.1016/j.enconman.2018.05.069.
[13] P. Gabrielli, M. Gazzani, M. Mazzotti, Electrochemical conversion technologies for optimal design of decentralized multi-energy systems: Modeling framework and technology assessment, Appl. Energy. 221 (2018) 557–575. doi:10.1016/j.apenergy.2018.03.149.
[14] D. Benouioua, D. Candusso, F. Harel, L. Oukhellou, Multifractal Analysis of Stack Voltage Based on Wavelet Leaders: A New Tool for PEMFC Diagnosis, Fuel Cells. 17 (2017) 217–224. doi:10.1002/fuce.201600029.
[15] E. Denisov, Y.K. Evdokimov, R.R. Nigmatullin, S. Martemianov, A. Thomas, N. Adiutantov, Spectral method for PEMFC operation mode monitoring based on electrical fluctuation analysis, Sci. Iran. 24 (2017) 1437–1447. doi:10.24200/sci.2017.4125.
[16] M.A. Rubio, K. Bethune, A. Urquia, J. St-Pierre, Proton exchange membrane fuel cell failure mode early diagnosis with wavelet analysis of electrochemical noise, Int. J. Hydrog. Energy. 41 (2016) 14991–15001. doi:10.1016/j.ijhydene.2016.05.292.
[17] E. Frappé, A. De Bernardinis, O. Bethoux, D. Candusso, F. Harel, C. Marchand, G. Coquery, PEM fuel cell fault detection and identification using differential method: simulation and experimental validation, Eur. Phys. J. Appl. Phys. 54 (2011) 23412. doi:10.1051/epjap/2011100277.
[18] Y.-H. Lee, S. Yoo, J. Kim, Development of Real-time Diagnosis Method for PEMFC Stack via Intermodulation Method, Trans. Korean Soc. Automot. Eng. 22 (2014) 76–83. doi:10.7467/KSAE.2014.22.7.076.
[19] EIS Diagnosis for PEM Fuel Cell Performance, in: Electrochem. Impedance Spectrosc. PEM Fuel Cells, Springer London, London, 2010: pp. 193–262. doi:10.1007/978-1-84882-846-9_5.
[20] E. Ramschak, V. Peinecke, P. Prenninger, T. Schaffer, W. Baumgartner, V. Hacker, Online stack monitoring tool for dynamically and stationary operated fuel cell systems, Fuel Cells Bull. 2006 (2006) 12–15. doi:10.1016/S1464-2859(06)71207-X.
[21] X.-Z. Yuan, C. Song, H. Wang, J. Zhang, Electrochemical Impedance Spectroscopy in PEM Fuel Cells, Springer London, London, 2010. doi:10.1007/978-1-84882-846-9.
[22] Y. Li, J. Yang, J. Song, Structure models and nano energy system design for proton exchange membrane fuel cells in electric energy vehicles, Renew. Sustain. Energy Rev. 67 (2017) 160–172. doi:10.1016/j.rser.2016.09.030.
[23] E.C. Kumbur, M.M. Mench, FUEL CELLS – PROTON-EXCHANGE MEMBRANE FUEL CELLS | Water Management, in: Encycl. Electrochem. Power Sources, Elsevier, 2009: pp. 828–847. doi:10.1016/B978-044452745-5.00862-5.
[24] A. Şahin, İ. Ar, Synthesis, characterization and fuel cell performance tests of boric acid and boron phosphate doped, sulphonated and phosphonated poly(vinyl alcohol) based composite membranes, J. Power Sources. 288 (2015) 426–433. doi:10.1016/j.jpowsour.2015.03.188.
[25] A. Ozden, M. Ercelik, Y. Devrim, C.O. Colpan, F. Hamdullahpur, Evaluation of sulfonated polysulfone/zirconium hydrogen phosphate composite membranes for direct methanol fuel cells, Electrochimica Acta. 256 (2017) 196–210. doi:10.1016/j.electacta.2017.10.002.
[26] M.J. Parnian, S. Rowshanzamir, A.K. Prasad, S.G. Advani, High durability sulfonated poly (ether ether ketone)-ceria nanocomposite membranes for proton exchange membrane fuel cell applications, J. Membr. Sci. 556 (2018) 12–22. doi:10.1016/j.memsci.2018.03.083.
[27] P. Mohanta, F. Regnet, L. Jörissen, Graphitized Carbon: A Promising Stable Cathode Catalyst Support Material for Long Term PEMFC Applications, Materials. 11 (2018) 907. doi:10.3390/ma11060907.
[28] J. Jang, J.G. Lee, H.J. Hwang, O. Kwon, O.S. Jeon, Y. Ji, Y.G. Shul, Role of Nitrogen-Doped Carbon Nanofibers Inside Polymer Membranes for Enhancing Fuel Cell Performance, Energy Technol. 6 (2018) 998–1002. doi:10.1002/ente.201700642.

[29] J. Maya-Cornejo, A. Garcia-Bernabé, V. Compañ, Bimetallic Pt-M electrocatalysts supported on single-wall carbon nanotubes for hydrogen and methanol electrooxidation in fuel cells applications, Int. J. Hydrog. Energy. 43 (2018) 872–884. doi:10.1016/j.ijhydene.2017.10.097.
[30] C. de Beer, P.S. Barendse, P. Pillay, B. Bullecks, R. Rengaswamy, Classification of High-Temperature PEM Fuel Cell Degradation Mechanisms Using Equivalent Circuits, IEEE Trans. Ind. Electron. 62 (2015) 5265–5274. doi:10.1109/TIE.2015.2393292.
[31] M. Pérez-Page, V. Pérez-Herranz, Study of the electrochemical behaviour of a 300 W PEM fuel cell stack by Electrochemical Impedance Spectroscopy, Int. J. Hydrog. Energy. 39 (2014) 4009–4015. doi:10.1016/j.ijhydene.2013.05.121.
[32] I. Pivac, B. Šimić, F. Barbir, Experimental diagnostics and modeling of inductive phenomena at low frequencies in impedance spectra of proton exchange membrane fuel cells, J. Power Sources. 365 (2017) 240–248. doi:10.1016/j.jpowsour.2017.08.087.
[33] J. Wysocka, S. Krakowiak, J. Ryl, K. Darowicki, Investigation of the electrochemical behaviour of AA1050 aluminium alloy in aqueous alkaline solutions using Dynamic Electrochemical Impedance Spectroscopy, J. Electroanal. Chem. 778 (2016) 126–136. doi:10.1016/j.jelechem.2016.08.028.
[34] J. Orlikowski, K. Darowicki, Investigations of pitting corrosion of magnesium by means of DEIS and acoustic emission, Electrochimica Acta. 56 (2011) 7880–7884. doi:10.1016/j.electacta.2010.12.021.
[35] A. Arutunow, K. Darowicki, DEIS evaluation of the relative effective surface area of AISI 304 stainless steel dissolution process in conditions of intergranular corrosion, Electrochimica Acta. 54 (2009) 1034–1041. doi:10.1016/j.electacta.2008.08.045.
[36] J. Ryl, K. Darowicki, P. Slepski, Evaluation of cavitation erosion–corrosion degradation of mild steel by means of dynamic impedance spectroscopy in galvanostatic mode, Corros. Sci. 53 (2011) 1873–1879. doi:10.1016/j.corsci.2011.02.004.
[37] P. Slepski, E. Janicka, A comprehensive analysis of impedance of the electrochemical cell, Russ. J. Electrochem. 50 (2014) 379–384. doi:10.1134/S1023193513090103.
[38] P. Slepski, K. Darowicki, E. Janicka, A. Sierczynska, Application of electrochemical impedance spectroscopy to monitoring discharging process of nickel/metal hydride battery, J. Power Sources. 241 (2013) 121–126. doi:10.1016/j.jpowsour.2013.04.039.
[39] P. Slepski, E. Janicka, K. Darowicki, B. Pierozynski, Impedance monitoring of fuel cell stacks, J. Solid State Electrochem. 19 (2015) 929–933. doi:10.1007/s10008-014-2676-8.
[40] K. Darowicki, E. Janicka, P. Slepski, Study of Direct Methanol Fuel Cell Process Dynamics Using Dynamic Electrochemical Impedance Spectroscopy, Int. J. Electrochem. Sci. 7 (2012) 12090–12097.
[41] European Stack Test project website. http://stacktest.zsw-bw.de/, 2015 (accessed 13 January 2018).
[42] J. Mitzel, E. Gülzow, A. Kabza, J. Hunger, S.S. Araya, P. Piela, I. Alecha, G. Tsotridis, Identification of critical parameters for PEMFC stack performance characterization and control strategies for reliable and comparable stack benchmarking, Int. J. Hydrog. Energy. 41 (2016) 21415–21426. doi:10.1016/j.ijhydene.2016.08.065.
[43] P. Slepski, K. Darowicki, E. Janicka, G. Lentka, A complete impedance analysis of electrochemical cells used as energy sources, J. Solid State Electrochem. 16 (2012) 3539–3549. doi:10.1007/s10008-012-1825-1.
[44] J. Wu, X.-Z. Yuan, J.J. Martin, H. Wang, FUEL CELLS – PROTON-EXCHANGE MEMBRANE FUEL CELLS | Life-Limiting Considerations, in: Encycl. Electrochem. Power Sources, Elsevier, 2009: pp. 848–867. doi:10.1016/B978-044452745-5.00894-7.
[45] M. Ciureanu, R. Roberge, Electrochemical Impedance Study of PEM Fuel Cells. Experimental Diagnostics and Modeling of Air Cathodes, J. Phys. Chem. B. 105 (2001) 3531–3539. doi:10.1021/jp003273p.

[46] S. Cruz-Manzo, R. Chen, P. Rama, Study of current distribution and oxygen diffusion in the fuel cell cathode catalyst layer through electrochemical impedance spectroscopy, Int. J. Hydrog. Energy. 38 (2013) 1702–1713. doi:10.1016/j.ijhydene.2012.08.141.
[47] F.J. Pinar, M. Rastedt, A. Dyck, P. Wagner, Long-term Operation of High Temperature Polymer Electrolyte Membrane Fuel Cells with Fuel Composition Switching and Oxygen Enrichment, Fuel Cells. 18 (2018) 260–269. doi:10.1002/fuce.201700115.
[48] P. Hong, J. Li, L. Xu, M. Ouyang, C. Fang, Modeling and simulation of parallel DC/DC converters for online AC impedance estimation of PEM fuel cell stack, Int. J. Hydrog. Energy. 41 (2016) 3004–3014. doi:10.1016/j.ijhydene.2015.11.129.
[49] R. Makharia, M.F. Mathias, D.R. Baker, Measurement of Catalyst Layer Electrolyte Resistance in PEFCs Using Electrochemical Impedance Spectroscopy, J. Electrochem. Soc. 152 (2005) A970. doi:10.1149/1.1888367.
[50] K. Wiezell, P. Gode, G. Lindbergh, Steady-State and EIS Investigations of Hydrogen Electrodes and Membranes in Polymer Electrolyte Fuel Cells, J. Electrochem. Soc. 153 (2006) A749. doi:10.1149/1.2172559.
[51] M.G. Hosseini, P. Zardari, Electrocatalytical study of carbon supported Pt, Ru and bimetallic Pt–Ru nanoparticles for oxygen reduction reaction in alkaline media, Appl. Surf. Sci. 345 (2015) 223–231. doi:10.1016/j.apsusc.2015.03.146.
[52] A.Z. Weber, R.L. Borup, R.M. Darling, P.K. Das, T.J. Dursch, W. Gu, D. Harvey, A. Kusoglu, S. Litster, M.M. Mench, R. Mukundan, J.P. Owejan, J.G. Pharoah, M. Secanell, I.V. Zenyuk, A Critical Review of Modeling Transport Phenomena in Polymer-Electrolyte Fuel Cells, J. Electrochem. Soc. 161 (2014) F1254–F1299. doi:10.1149/2.0751412jes.
[53] T.E. Springer, Characterization of Polymer Electrolyte Fuel Cells Using AC Impedance Spectroscopy, J. Electrochem. Soc. 143 (1996) 587. doi:10.1149/1.1836485.
[54] K. Darowicki, L. Gawel, Impedance Measurement and Selection of Electrochemical Equivalent Circuit of a Working PEM Fuel Cell Cathode, Electrocatalysis. 8 (2017) 235–244. doi:10.1007/s12678-017-0363-0.
[55] M.E. Orazem, B. Tribollet, Electrochemical Impedance Spectroscopy: Orazem/Electrochemical, John Wiley & Sons, Inc., Hoboken, NJ, USA, 2008. doi:10.1002/9780470381588.ch19.
[56] D. Conteau, C. Bonnet, D. Funfschilling, M. Weber, S. Didierjean, F. Lapicque, Detection of Liquid Water in PEM Fuel Cells' Channels: Design and Validation of a Microsensor, Fuel Cells. 10 (2010) 520–529. doi:10.1002/fuce.200900167.

Figures captions:

Fig. 1 PEMFC stack scheme and DEIS measurement principle.

Fig. 2 a) I-V Characteristic of stack with 3 distinguished regions b) I-V Characteristics of each individual cell c) DEIS graph for stack d) Comparison of DEIS results for cell no. 1 (faulty, black line) and cell no. 7 (healthy, blue line). Scanning current rate di/dt=20 mA s^{-1}.

Fig. 3 Comparison of DEIS results of cell no. 1 and cell no. 7 for the following current ranges a) 0 - 0.1 A cm^{-2} b) 0.1 - 0.6 A cm^{-2} c) 0.6 – 1 A cm^{-2}. Scanning current rate di/dt=20 mA s^{-1}.

Fig. 4 Five equivalent circuits used for statistical comparison of χ^2 parameter (see paragraph 3.2 for further explanation). Meaning of the symbols used is as follows: resistance  , capacitance  , constant phase element  , semi infinite Warburg impedance ,open finite-length diffusion impedance  .

- Dynamic impedance measurements simultaneously on stack and single cell level
- New diagnostics method of PEM fuel cells in real operating conditions
- Detection of malfunction cell with fault characterisation
- The best statistical equivalent circuit for whole range of operations

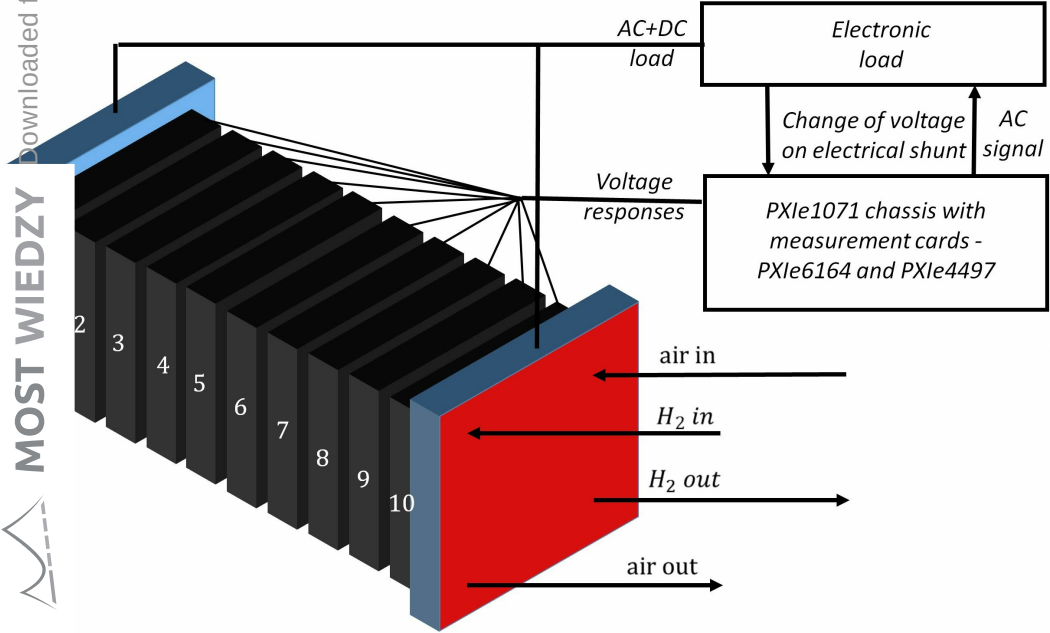

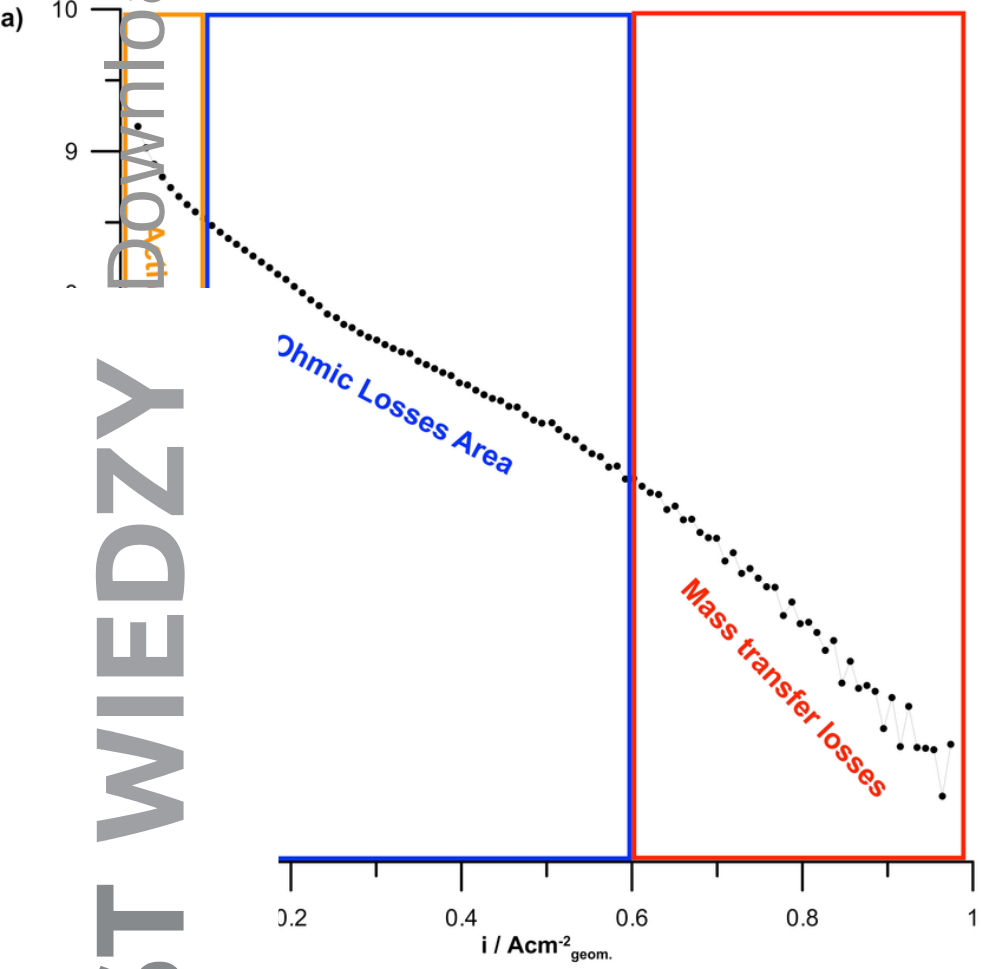

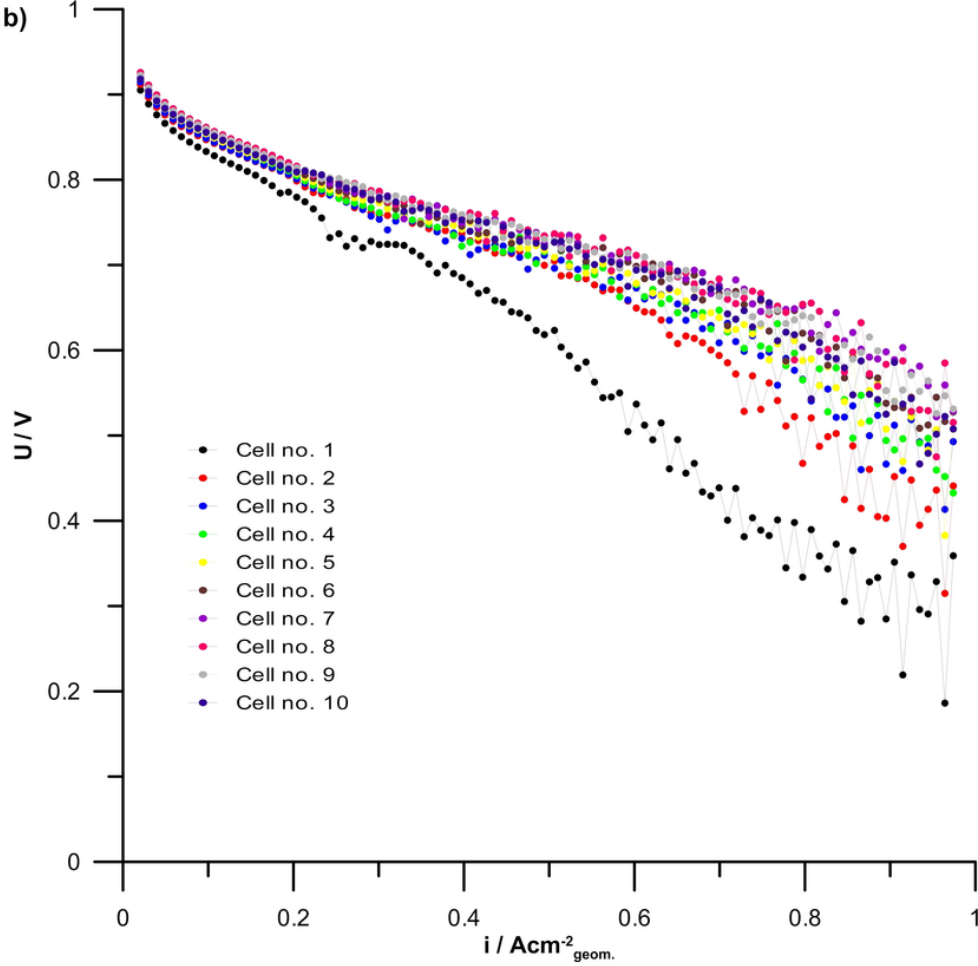

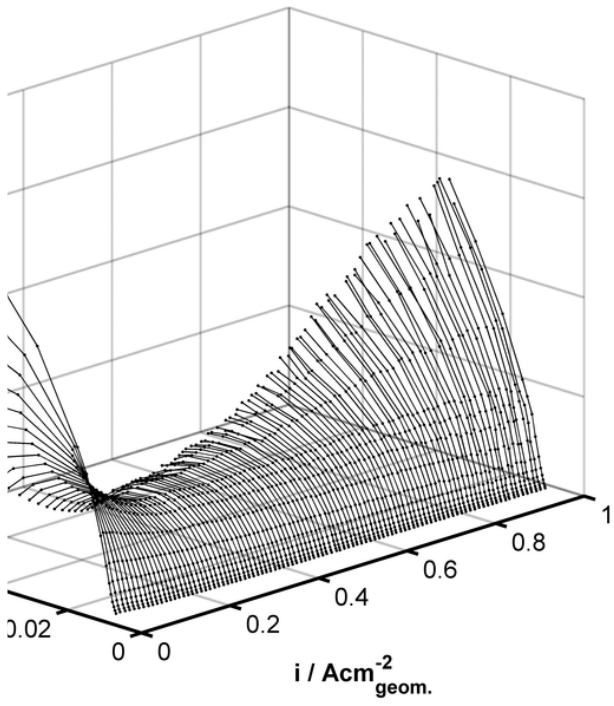

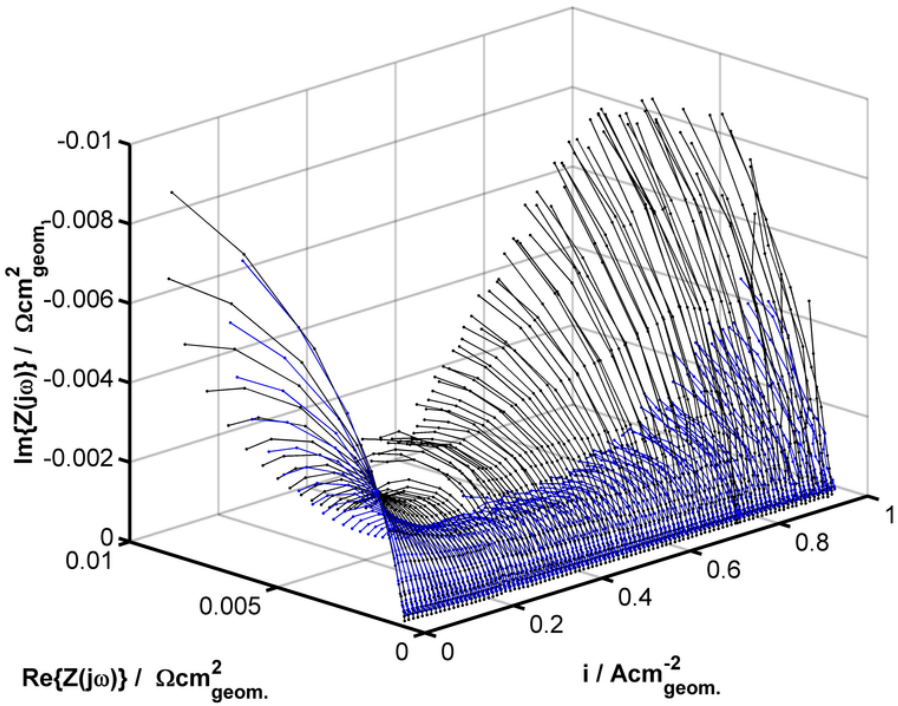

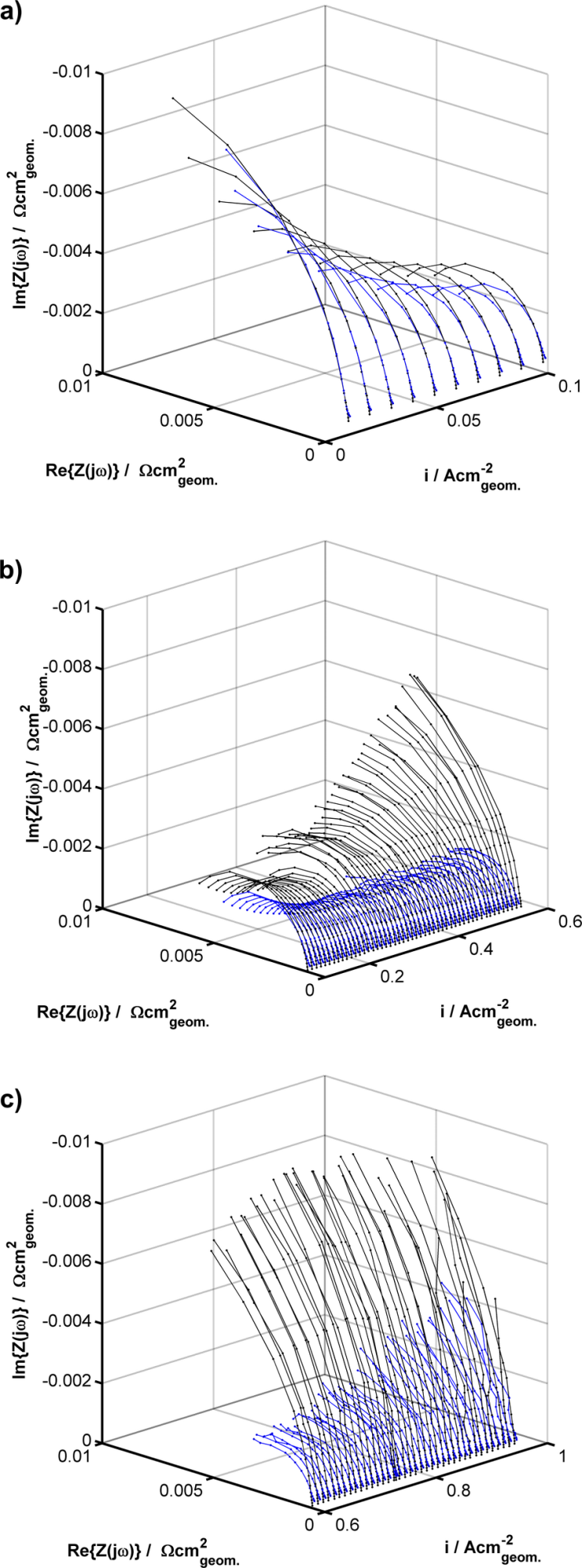
a)
-0.01
-0.008
-0.006
-0.004
-0.002
0
Im{Z(jω)} / Ωcm²geom.
0.01
0.005
0
Re{Z(jω)} / Ωcm²geom.
0
0.05
0.1
i / Acm⁻²geom.
b)
-0.01
-0.008
-0.006
-0.004
-0.002
0
Im{Z(jω)} / Ωcm²geom.
0.01
0.005
0
Re{Z(jω)} / Ωcm²geom.
0.2
0.4
0.6
i / Acm⁻²geom.
c)
-0.01
-0.008
-0.006
-0.004
-0.002
0
Im{Z(jω)} / Ωcm²geom.
0.01
0.005
0
Re{Z(jω)} / Ωcm²geom.
0.6
0.8
1
i / Acm⁻²geom.